# Influence of temperature-dependent density inhomogeneity on the stability of atmospheric stratified fluids

T. D. Kaladze[1, *] and A. P. Misra[2, †]

[1] *I. Vekua Institute of Applied Mathematics and E. Andronikashvili Institute of Physics, Tbilisi State University, Georgia*
[2] *Department of Mathematics, Siksha Bhavana, Visva-Bharati University, Santiniketan-731 235, India*

The stability of atmospheric stratified fluids is revisited to study the influence of the temperature-dependent density inhomogeneity due to thermal expansion in the Earth's lower atmosphere (with heights 0 to 50 km) under the action of gravity. Previous theory in the literature [Phys. Lett. A 480 (2023) 128990] is modified and advanced. It is found that the Brunt-Väisälä frequency associated with internal gravity waves is modified, leading to new instability conditions of vertically stratified fluids. The possibility of the onset of Rayleigh-Bénard convective instability is also discussed, and the influences of the modified Brunt-Väisälä frequency and the density and temperature gradients on the instability growth rates are studied.

## I. INTRODUCTION

Continued global warming and climate change deserve great interest from scientists studying problems of atmospheric circulation dynamics, e.g., problems describing free thermal convection [1]. Such motions, which arise in the gravity field at spatial inhomogeneity of density caused by temperature inhomogeneity were intensively discussed. Acheson and Hide [2] noted that differential heating produces temperature variations from place to place, and owing to thermal expansion, they give rise to density stratification, causing so-called thermal instabilities. In [3], the effect of a small-scale helical driving force on fluid with a stable vertical temperature gradient, with a small Reynolds number, under the action of gravity is considered. The authors showed large-scale vortex instability in the fluid despite its stable stratification. At a nonlinear stage, this instability gives many stationary spiral vortex structures. Among these structures, there is a stationary helical soliton and a kink of the new type. Later in [4], authors considered stratified in gravity field rotating flow and found a new large-scale instability. They obtained nonlinear equations for the instability and gave a detailed study of the linear stage of the instability and the conditions of its appearance. They noted that instability is possible in the case of both stable and unstable vertical temperature stratifications. The authors in [5] reported a new type of large-scale instability generated by the unstable vertical temperature gradient (heated from below) and small-scale force with zero helicity in an inclined rotating fluid with solutions in localized vortex kink-like structures. Such investigations dealt with the propagation problems of internal gravity waves [6]. In Ref. [7], the authors discussed vertical coupling in the atmosphere and ionosphere system by internal waves generated in the lower atmosphere. In addition, they also discussed the progress in the sudden stratospheric warming and upper atmospheric circulation due to wave-induced vertical coupling between the lower and upper atmosphere.

Recently, Kaladze and Misra [8] studied the influences of the temperature and density gradients due to thermal expansion on the stability of vertically stratified fluids in the Earth's atmosphere. The authors initiated an investigation in the atmospheric layer ($0 < z < 50$ km heights) with negative and positive vertical temperature gradients in the tropospheric ($0 < z < 15$ km) and stratospheric $15 < z < 50$ km) regions separately. They showed that such influence could lead to instability in stratified incompressible fluids. They also obtained the Brunt-Väisälä frequency modified by the thermal expansion coefficient and the critical value of the expansion coefficient for which the instability of internal gravity waves occurs. In their approach, they ignored the dependence of the background density of stratified fluids on the variation of the background fluid temperature. However, spatial variations of fluid temperatures in the atmosphere can cause density variations owing to the thermal expansion [2]. Such temperature dependence can significantly influence the spatio-temporal evolution of perturbed flows. Thus, it becomes necessary to take into account such effects in the dynamics of stratified atmospheric fluids.

In this work, we consider such density inhomogeneity effect due to temperature variation and the vertical temperature gradient with an arbitrary sign, which allows the expansion of atmospheric layers with heights ranging from 0 to 50 km and to consider arbitrary length scales of density and temperature inhomogeneities. In this way, we modify and advance the work by Kaladze and Misra [8]. We show that the Brunt-Väisälä frequency associated with the internal gravity waves (IGWs) gets modified by this effect, and we obtain new instability conditions for IGWs. Consequently, the Rayleigh-Bénard convective instability and the modified instability growth rate occur.

* tamaz˙kaladze@yahoo.com
† Author to whom correspondence should be addressed; apmisra@visva-bharati.ac.in

## II. MODELING OF DENSITY INHOMOGENEITY DUE TO THERMAL EXPANSION

Typically, differential heating causes atmospheric convection in which the spatial variation of temperature may lead to the density variation due to the thermal expansion of stratified fluids. So, modeling of the density inhomogenity due to temperature variation is necessary for atmospheric fluid dynamics. To this end, we consider the following equation of state for incompressible atmospheric fluids, i.e., the dependence of the fluid density ($\rho$) on the fluid temperature ($T$) and pressure ($p$).

$$\rho = \rho(T, p). \tag{1}$$

Any physical state variable, $f$ can be considered as the superposition of the mean (background) state and the perturbed state, i.e., $f = \overline{f} + f'$, where the choice of the mean $\overline{f}$ plays a crucial role for the spatio-temporal evolution of the perturbation $f'$. Next, we consider the Taylor-series expansion of $\rho$ about the unperturbed or mean state $\overline{\rho}(z) \equiv \overline{\rho}\left(\overline{T}(z), \overline{p}(z)\right)$ and assume that the deviations of the fluid density, pressure, and temperature from the unperturbed (background or mean) state are small. Thus, we obtain from Eq. (1) the following expansion for $\rho$ to the first-order-smallness of perturbations.

$$\begin{aligned} \rho(\mathbf{r}, t) &= \overline{\rho}(z) + \rho'(\mathbf{r}, t) \\ &= \overline{\rho}(z)\left[1 - \beta T'(\mathbf{r}, t) + \alpha p'(\mathbf{r}, t)\right], \end{aligned} \tag{2}$$

where $\mathbf{r} = (x, y, z)$ and the expansion coefficients associated with the temperature and pressure, respectively, are

$$\beta = -\frac{1}{\overline{\rho}}\left(\frac{\partial \rho}{\partial T}\right)_p, \ \alpha = \frac{1}{\overline{\rho}}\left(\frac{\partial \rho}{\partial p}\right)_T. \tag{3}$$

The negative sign in $\beta$ is considered to mean that the fluid density increases with decreasing the temperature at atmospheric heights. The smallness of the perturbed density relative to its unperturbed state requires to fulfill the following condition:

$$|\beta T' - \alpha p\prime| \ll 1. \tag{4}$$

Typically, the thermal expansion coefficient, $\beta$ is small ($\ll 1$), and it decreases with increasing the temperature [8]. So, the condition (4) gives

$$|\beta T'| \ll 1, \quad |\alpha p\prime| \ll 1. \tag{5}$$

Next, we assume that the fluid density variation due to the pressure inhomogeneity is small compared to the temperature inhomogeneity, i.e.,

$$|\alpha p'| \ll |\beta T'|. \tag{6}$$

Such an assumption is valid for atmospheric stratified fluids. Thus, ignoring the term proportional to $\alpha$, Eq. (2) reduces to

$$\rho(\mathbf{r}, t) \equiv \overline{\rho}(z) + \rho'(\mathbf{r}, t) = \overline{\rho}(z)\left[1 - \beta T'(\mathbf{r}, t)\right], \tag{7}$$

where the perturbed density $\rho'$ is given by

$$\rho'(\mathbf{r}, t) = -\overline{\rho}(z)\beta T'. \tag{8}$$

However, the density variation due to temperature can not be neglected as it gives rise to the fluid convective motion. The condition (6) means that the pressure of the stratified fluids does not change drastically. In particular, it follows that the vertical scale of area where the convection occurs may not be too large. If the characteristic vertical scale is $L$, then the hydrostatic change of pressure has the order $\overline{\rho} g L$, i.e., $|p_1' - p_2'| \sim \overline{\rho} g L$, where $g$ is the constant acceleration due to gravity acting vertically downwards and the conditions (5) and (6) give

$$\overline{\rho} g L |\alpha| \ll |\beta| \theta \ll 1, \tag{9}$$

where $\theta = |T_1' - T_2'|$ is the characteristic temperature difference.

## III. BASIC EQUATIONS

We consider the dynamics of incompressible stratified neutral fluids in the lower atmosphere (with heights $0 < z < 50$ km) under the action of the gravity force $\mathbf{g} = (0, 0, -g)$ per unit fluid mass density directed vertically downward. Our starting point is the following Navier-Stokes equation for incompressible neutral fluids.

$$\rho\left[\frac{\partial \mathbf{v}}{\partial t} + (\mathbf{v} \cdot \nabla)\mathbf{v}\right] = -\nabla p + \rho \mathbf{g} + \mu \nabla^2 \mathbf{v}, \tag{10}$$

where $\mathbf{v}$ is the neutral fluid velocity and $\mu$ is the coefficient of the fluid dynamic viscosity. The hydrostatic equilibrium state of fluid flow with $\mathbf{v} = 0$ can be described from Eq. (10) as

$$0 = -\frac{1}{\overline{\rho}}\nabla \overline{p} + \mathbf{g}. \tag{11}$$

It is well known that the Boussinesq approximation is used to study convective motions or buoyancy-driven flows or gravity waves originating from the buoyancy force that are slower than typical sound waves in incompressible fluids. In this approximation, the kinematic viscosity coefficient is assumed to be constant, the density differences (due to inertial effects) are ignored except for the term associated with the gravity, and the density is solely a function of temperature. Thus, noting that $\rho$ behaves as the local fluid density and $\overline{\rho}$ as the reference density, and using the Boussinesq approximation and Eq. (11), we obtain from Eq. (10) the following reduced equation for the perturbed fluid velocity $\mathbf{v}$ (without using prime symbol for $\mathbf{v}$, for simplicity).

$$\frac{\partial \mathbf{v}}{\partial t} + (\mathbf{v} \cdot \nabla)\mathbf{v} = -\frac{1}{\overline{\rho}}\nabla p' + \beta T' g \hat{z} + \nu \nabla^2 \mathbf{v}, \tag{12}$$

where we have substituted $\rho' = -\beta \overline{\rho} T'$ from Eq. (8) and the term proportional to $\beta$ represents the buoyancy force.

Also, $\nu = \mu/\overline{\rho}$ is the coefficient of the fluid kinematic viscosity and $\hat{z}$ is the unit vector along the positive $z$-axis (vertically upward). The momentum balance equation (12) is to be closed by the following continuity equation and the heat equation in absence of any heat source for the perturbed velocity $\mathbf{v}$ and temperature $T'$.

$$\nabla \cdot \mathbf{v} = 0, \tag{13}$$

$$\frac{\partial T'}{\partial t} + (\mathbf{v}\cdot\nabla)(\overline{T}+T') = \chi\nabla^2(\overline{T}+T'), \tag{14}$$

where $\chi$ is the coefficient of the thermal diffusivity. In Eq. (13), we have used the following condition for incompressible fluids.

$$\frac{d\rho}{dt} \equiv \frac{\partial \rho}{\partial t} + \mathbf{v}\cdot\nabla\rho = 0. \tag{15}$$

Next, from the basic state (unperturbed state) of heat equation (14), we have $d^2\overline{T}/dz^2 = 0$, which gives $d\overline{T}/dz = C_0$, a constant, and hence the following linear vertical temperature distribution.

$$\overline{T}(z) = C_0 z + C_1, \tag{16}$$

where $C_1$ is another constant of integration. Applying this result to Eq. (14), we have

$$\frac{\partial T'}{\partial t} + (\mathbf{v}\cdot\nabla)T' + C_0 w = \chi\nabla^2 T', \tag{17}$$

where $\mathbf{v} \equiv (u, v, w) = \mathbf{v}_\perp + w\hat{z}$. Furthermore, we recast Eq. (15) in the following reduced form.

$$w\frac{d\overline{\rho}}{dz} + \frac{d\rho'}{dt} = 0. \tag{18}$$

Equations (12), (13), (17), and (18) are the desired set of equations for the dynamics of atmospheric stratified incompressible fluid flows. Comparing these equations with those in [8], we note that not only the effect of fluid viscosity is considered in addition to the present work, the temperature (unperturbed) gradient ($C_0$) appears to be constant in contrast to the work [8].

## IV. BRUNT-VÄISÄLÄ FREQUENCY AND INSTABILITY CONDITION

To explicate the roles of the density gradient and the vertical temperature gradient, we consider a simple case, i.e., the linear flow of nonviscous fluids. Thus, separating the perpendicular and vertical (along the $z$-axis) components of the fluid velocity in Eq. (12), we obtain

$$\frac{\partial \mathbf{v}_\perp}{\partial t} + \frac{1}{\overline{\rho}}\nabla_\perp p' = 0, \tag{19}$$

$$\frac{\partial w}{\partial t} + \frac{1}{\overline{\rho}}\frac{\partial p'}{\partial z} - g\beta T' = 0. \tag{20}$$

Also, the equation of continuity (13) gives

$$\nabla_\perp \cdot \mathbf{v}_\perp = -\frac{\partial w}{\partial z}. \tag{21}$$

Taking divergence of Eq. (19), noting that $\nabla_\perp^2 = \Delta_\perp = \partial^2/\partial x^2 + \partial^2/\partial y^2$, and using Eq. (21), we obtain

$$\frac{\partial^2 w}{\partial t\partial z} = \frac{1}{\overline{\rho}}\nabla_\perp^2 p'. \tag{22}$$

Next, using the operator $\partial\Delta_\perp/\partial t$ to Eq. (20) we get

$$\frac{\partial^2}{\partial t^2}\Delta_\perp w + \frac{1}{\overline{\rho}}\frac{\partial^2}{\partial t\partial z}\Delta_\perp p' - g\beta\frac{\partial}{\partial t}\Delta_\perp T' = 0. \tag{23}$$

Also, using Eq. (22) and noting that $\overline{\rho} = \overline{\rho}(z)$, Eq. (23) reduces to

$$\frac{\partial^2}{\partial t^2}\left(\Delta w + \frac{1}{\overline{\rho}}\frac{d\overline{\rho}}{dz}\frac{\partial w}{\partial z}\right) - g\beta\frac{\partial}{\partial t}\Delta_\perp T' = 0, \tag{24}$$

where $\Delta = \Delta_\perp + \partial^2/\partial z^2$ is the Laplacian operator.

In what follows, we operate Eq. (17) with $\Delta_\perp$ to get in the linear approximation,

$$\frac{\partial}{\partial t}\Delta_\perp T' = \chi\Delta_\perp\Delta T' - C_0\Delta_\perp w. \tag{25}$$

Combining Eqs. (24) and (25), we have

$$\frac{\partial^2}{\partial t^2}\left(\Delta w + \frac{1}{\overline{\rho}}\frac{d\overline{\rho}}{dz}\frac{\partial w}{\partial z}\right) - g\beta\chi\Delta_\perp\Delta T' + gC_0\beta\Delta_\perp w = 0. \tag{26}$$

Using the relation for the perturbed density, $\rho' = -\overline{\rho}(z)\beta T'$ [Eq. (8)] to Eq. (18), we obtain

$$(1-\beta T')\frac{1}{\overline{\rho}}\frac{d\overline{\rho}}{dz}w - \beta\frac{dT'}{dt} = 0. \tag{27}$$

Next, using Eq.(17) to Eq. (27), in the linear approximation, we obtain

$$\frac{1}{\overline{\rho}}\frac{d\overline{\rho}}{dz}w - \beta\chi\Delta T' + C_0\beta w = 0. \tag{28}$$

Finally, from Eqs. (26) and (28), we obtain the following evolution equation for stratified incompressible fluid flows in the lower atmosphere.

$$\frac{\partial^2}{\partial t^2}\left(\Delta w + \frac{1}{\overline{\rho}}\frac{d\overline{\rho}}{dz}\frac{\partial w}{\partial z}\right) + N^2(z)\Delta_\perp w = 0, \tag{29}$$

where $N^2$ is the squared Brunt-Väisälä frequency, given by,

$$N^2(z) = -\frac{1}{\overline{\rho}}\frac{d\overline{\rho}}{dz}g. \tag{30}$$

Equation (29) has the same form as for ordinary internal gravity waves [9, 10] in absence of the effects of thermal expansion. It is important to note that the choice of the mean fluid density (background) is crucial for the spatio-temporal evolution of the perturbed fluid velocity $w$. Since the temperature variation in the Earth's atmosphere can cause the density variation due to thermal expansion, we model the background density $\overline{\rho}(z) \equiv \overline{\rho}\left(\overline{T}(z), \overline{p}(z)\right)$ as [2]

$$\overline{\rho}(z) = \rho_0(z)\left[1 - \beta\left(\overline{T}(z) - T_0\right)\right], \tag{31}$$

where $\rho_0(z)$ is the fluid mass density at some reference temperature, $\overline{T}(z) = T_0$ at a particular height, applicable for ordinary internal gravity waves. In view of the assumption (31), the expression (30) for the Brunt-Väisälä frequency reduces to

$$\begin{aligned} N^2(z) =& \frac{g}{1-\beta\mathcal{T}}\times \\ &\left[(\beta\mathcal{T}-1)\frac{1}{\rho_0}\frac{d\rho_0}{dz} + \beta\frac{d\overline{T}}{dz}\right], \\ =& -g\left(\frac{1}{\rho_0}\frac{d\rho_0}{dz} - \frac{\beta\mathcal{T}}{1-\beta\mathcal{T}}\frac{1}{\mathcal{T}}\frac{d\mathcal{T}}{dz}\right), \end{aligned} \tag{32}$$

where $\rho_0 \equiv \rho_0(z)$, $\mathcal{T} \equiv \mathcal{T}(z) = \overline{T}(z) - T_0$. Comparing the first form of Eq. (32) with Eq. (21) of Ref. [8], we find that an additional factor $1 - \beta\mathcal{T}(z)$ appears in Eq. (32) before the square brackets due to the modeling of the background density with thermal expansion effects [*cf.* Eq. (31)]. Furthermore, in contrast to Ref. [8], the temperature gradient $C_0 \equiv d\overline{T}(z)/dz$ is no longer varying but a constant [*cf.* Eq. (16)].

In what follows, we obtain the instability conditions from Eq. (32), and note that $d\rho_0/dz < 0$ holds in the atmospheric heights $0 < z < 50$ km [8] and $\beta\mathcal{T} < 1$ holds good as per the assumption (9). Furthermore, $d\mathcal{T}/dz < 0$ in the tropospheric heights $0 < z < 15$ km and $d\mathcal{T}/dz > 0$ in the stratospheric heights $15 < z < 50$ km [8]. So, in the tropospheric layer, the necessary conditions for the instability at which $N^2 < 0$ are $\beta\mathcal{T} < 1$ and $d\mathcal{T}/dz < 0$. On the other hand, since the conditions $d\mathcal{T}/dz > 0$ and $\beta\mathcal{T} < 1$ are likely to hold in the stratosphere, the fluid is said to be stable there for $N^2 > 0$. The sufficient condition of instability gives

$$\left(\frac{1}{\rho_0}\frac{d\rho_0}{dz} > \frac{\beta\mathcal{T}}{1-\beta\mathcal{T}}\frac{1}{\mathcal{T}}\frac{d\mathcal{T}}{dz}\right). \tag{33}$$

Since as said before, $d\rho_0/dz < 0$ in the atmospheric region of heights $0 < z < 50$ km and $\beta\mathcal{T} < 1$ as per the assumption (9), the condition (33) can only be satisfied when $d\mathcal{T}/dz < 0$. Typically, the length scale of the temperature inhomogeneity is larger than that of the density inhomogeneity [8], i.e.,

$$L_{\mathcal{T}}^{-1} \equiv \frac{1}{\mathcal{T}}\left|\frac{d\mathcal{T}}{dz}\right| < L_{\rho_0}^{-1} \equiv \frac{1}{\rho_0}\left|\frac{d\rho_0}{dz}\right|. \tag{34}$$

So, by means of the relation (34), Eq. (33) reduces to

$$1 < \left|\frac{L_{\mathcal{T}}}{L_{\rho_0}}\right| < \frac{\beta\mathcal{T}}{1-\beta\mathcal{T}}. \tag{35}$$

The condition (35) is satisfied only when $0.5 \lesssim \beta\mathcal{T} \lesssim 1$, which is rather a harsh one in the atmospheric regions. Thus, we may conclude that incompressible stratified fluid flows may be unstable in the tropospheric layer $0 < z < 15$ km but stable in the other region, i.e., $15 < z < 50$ km. For typical values of the atmospheric fluid density $\rho_0(z)$ and temperature $\overline{T}$, and their gradients, readers are referred to the work of Kaladze and Misra [8].

## V. RAYLEIGH-BÉNARD CONVECTIVE INSTABILITY

As an illustration, we consider the possible convective instability in the tropospheric layer with negative vertical temperature gradient, i.e., $d\mathcal{T}/dz < 0$. We assume that such layer spans between heights $z_0 = 0$ km and $z_1 = 15$ km. The temperatures at the bottom and top boundaries are kept fixed at $T = T_0$ at $z_0 = 0$ km and at $T = T_1$ at $z_1 = 15$ km, so that the temperature at the top boundary is lower than the bottom boundary, i.e., $\Delta T = T_0 - T_1 > 0$.

As a starting point, we consider Eqs. (12), (13), and Eq. (17), and recast them in linearized forms as

$$\left(\frac{\partial}{\partial t} - \nu\nabla^2\right)u = -\frac{1}{\overline{\rho}}\frac{\partial p'}{\partial x}, \tag{36}$$

$$\left(\frac{\partial}{\partial t} - \nu\nabla^2\right)v = -\frac{1}{\overline{\rho}}\frac{\partial p'}{\partial y}, \tag{37}$$

$$\frac{\partial w}{\partial t} = -\frac{1}{\overline{\rho}}\frac{\partial p'}{\partial z} + \beta g T' + \nu\nabla^2 w, \tag{38}$$

$$\frac{\partial u}{\partial x} + \frac{\partial v}{\partial y} + \frac{\partial w}{\partial z} = 0, \tag{39}$$

$$\frac{\partial T'}{\partial t} - \Gamma w = \chi\nabla^2 T', \tag{40}$$

where we have obtained the first three equations [(36) to (38)] from Eq. (12) after separating the velocity components along the axes and $\Gamma = -C_0 = -d\overline{T}/dz > 0$ is so called the lapse rate.

Eliminating $T'$ from Eqs. (38) and (40), we get

$$\begin{aligned} &\left[\left(\frac{\partial}{\partial t} - \chi\Delta\right)\left(\frac{\partial}{\partial t} - \nu\Delta\right) - \beta g\Gamma\right]w = \\ &-\left(\frac{\partial}{\partial t} - \chi\Delta\right)\frac{1}{\overline{\rho}}\frac{\partial p'}{\partial z}. \end{aligned} \tag{41}$$

Differentiating Eqs. (36) and (37) with respect to $x$ and $y$ successively and using the results for $\partial u/\partial x$ and $\partial v/\partial y$ in Eq. (39), we obtain

$$\left(\frac{\partial}{\partial t} - \nu\Delta\right)\frac{\partial w}{\partial z} = \frac{1}{\overline{\rho}}\Delta_\perp p'. \tag{42}$$

Next, differentiating Eq. (41) with respect to $z$ we get

$$\begin{aligned}&\left[\left(\frac{\partial}{\partial t}-\chi\Delta\right)\left(\frac{\partial}{\partial t}-\nu\Delta\right)-\beta g\Gamma\right]\frac{\partial w}{\partial z}=\\&-\left(\frac{\partial}{\partial t}-\chi\Delta\right)\frac{\partial}{\partial z}\left(\frac{1}{\overline{\rho}}\frac{\partial p'}{\partial z}\right).\end{aligned}\tag{43}$$

Further applying the operator $\partial/\partial t-\nu\nabla^2$ to Eq. (43) and using Eq. (42), we obtain

$$\begin{aligned}&\left[\left(\frac{\partial}{\partial t}-\chi\Delta\right)\left(\frac{\partial}{\partial t}-\nu\Delta\right)-\beta g\Gamma\right]\frac{1}{\overline{\rho}}\Delta_\perp p'=\\&-\left(\frac{\partial}{\partial t}-\chi\Delta\right)\left(\frac{\partial}{\partial t}-\nu\Delta\right)\frac{\partial}{\partial z}\left(\frac{1}{\overline{\rho}}\frac{\partial p'}{\partial z}\right),\end{aligned}\tag{44}$$

or,

$$\begin{aligned}&\left[\left(\frac{\partial}{\partial t}-\chi\Delta\right)\left(\frac{\partial}{\partial t}-\nu\Delta\right)-\beta g\Gamma\right]\frac{1}{\overline{\rho}}\Delta_\perp p'=\\&-\left(\frac{\partial}{\partial t}-\chi\Delta\right)\left(\frac{\partial}{\partial t}-\nu\Delta\right)\left(\frac{1}{\overline{\rho}}\frac{\partial^2 p'}{\partial z^2}-\frac{1}{\overline{\rho}^2}\frac{d\overline{\rho}}{dz}\frac{\partial p'}{\partial z}\right),\end{aligned}\tag{45}$$

and finally we obtain the following equation.

$$\begin{aligned}&\left(\frac{\partial}{\partial t}-\chi\Delta\right)\left(\frac{\partial}{\partial t}-\nu\Delta\right)\frac{\Delta p'}{\overline{\rho}}-\beta g\Gamma\frac{1}{\overline{\rho}}\Delta_\perp p'=\\&\left(\frac{\partial}{\partial t}-\chi\Delta\right)\left(\frac{\partial}{\partial t}-\nu\Delta\right)\frac{1}{\overline{\rho}^2}\frac{d\overline{\rho}}{dz}\frac{\partial p'}{\partial z}.\end{aligned}\tag{46}$$

We assume that the charateristic size of variation of $\overline{\rho}(z)$ is much larger than that for $p'$. In this situation, $\overline{\rho}$ may be considered as a constant and we can recast Eq. (46) as

$$\begin{aligned}&\left(\frac{\partial}{\partial t}-\chi\Delta\right)\left(\frac{\partial}{\partial t}-\nu\Delta\right)\Delta p'-\beta g\Gamma\Delta_\perp p'=\\&-\frac{1}{g}\left(\frac{\partial}{\partial t}-\chi\Delta\right)\left(\frac{\partial}{\partial t}-\nu\Delta\right)N^2\frac{\partial p'}{\partial z},\end{aligned}\tag{47}$$

where $N^2$ is the Brunt-Väisälä frequency given by Eq. (30).

To reveal the role of the term proportional to $N^2$ on the wave dynamics, we assume that the length scale of fluid density inhomogeneity remains approximately a constant, i.e., $1/L_{\rho_0}\equiv(1/\rho_0)(d\rho_0/dz)$ is constant and so is $N^2$. The latter can assume a negative sign for the instability to occur (See Sec. IV). Next, to study the characteristics of the wave eigenmode, we assume the perturbations to propagate as plane waves with wave vector $\mathbf{k}=(k_x,k_y,k_z)=\mathbf{k}_\perp+k_z\hat{z}$ and wave frequency $\omega$ with constant amplitude $\tilde{p}$ in the following form:

$$p'(\mathbf{r},t)=\tilde{p}\exp\left(i\mathbf{k}\cdot\mathbf{r}-i\omega t\right).\tag{48}$$

Substitution of Eq. (48) into Eq. (47) yields the following dispersion relation for Rayleigh-Bénard convective flows.

$$\left(k^2-i\frac{N^2}{g}k_z\right)\left[\omega^2+i(\chi+\nu)k^2\omega-\chi\nu k^4\right]+\beta g\Gamma k_\perp^2=0.\tag{49}$$

In particular, in absence of the effects of fluid viscosity and thermal diffusivity, i.e., $\nu=0,\ \chi=0$, Eq. (49) gives the following expressions for the real ($\omega_r=\Re\omega$) and the imaginary ($\gamma=\Im\omega$) parts of the wave frequency $\omega$.

$$\omega_r=\pm\frac{1}{\sqrt{2}}\frac{\sqrt{\beta g\Gamma}k_\perp}{K_N}\left(1-\frac{k^2}{K_N^2}\right)^{1/2},\tag{50}$$

$$\gamma=\mp\frac{1}{\sqrt{2}}\sqrt{\frac{\beta\Gamma}{g}}N^2\frac{k_\perp k_z}{K_N^3}\left(1-\frac{k^2}{K_N^2}\right)^{-1/2},\tag{51}$$

where $\omega_r$ and $\gamma$ are related to

$$\omega_r\gamma=-\beta\Gamma N^2\frac{k_\perp^2 k_z}{K_N^4},\tag{52}$$

and $K_N=\left(k^4+N^4k_z^2/g^2\right)^{1/4}$. From Eqs. (50) and (51), we note that for $N^2<0$ and $k_z>0$, we have the instability ($\gamma>0$) and a real wave mode propagating vertically upwards in the atmosphere with the frequency $\omega_r$ ($>0$). Typically, for a particular atmospheric model, $|N^2|\sim 10^{-4}-10^{-3}/\mathrm{s}^2$ and $g\sim 10$ m/s$^2$ [8] so that $K_N\approx k$ for $k_z\ll 1$ such that $\omega_r\approx 0$. However, for moderate values of $|N^2|$ and $k_z$, such an approximation may not be valid. Thus, in this approximation and in absence of the effects of fluid viscosity and thermal diffusivity, the Rayleigh-Bénard convective flows with positive lapse rate $\Gamma$ can no longer propagate with a finite wave frequency $\omega_r$, but can have a finite growth rate of instability, given by,

$$|\gamma|\approx\sqrt{\beta g\Gamma}\frac{k_\perp}{k}.\tag{53}$$

Clearly, the instability grows and the instability growth rate increases with increasing values of the thermal coefficient $\beta$ and the thermal lapse rate $\Gamma$ without any cut-off unless $k_\perp=0$. Since the thermal lapse rate remains a constant, the increasing values of $\beta$ may correspond to the region of low-temperatures with heights ranging from 0 to 15 km (See, e.g., Table 1 of Ref. [8]).

On the other hand, if the dissipation due to thermal diffusion dominates over the time evolution of perturbation, the term $\omega^2$ can be neglected compared to the terms proportional to $\chi$. Thus, for a non-viscous ($\nu=0$) slowly varying perturbations, Eq. (49) gives, after separating the real and imaginary parts, the following wave frequency and the growth rate.

$$\omega_r=-\frac{\beta\Gamma N^2}{\chi K_N^4}\frac{k_\perp^2}{k^2}k_z,\tag{54}$$

$$\gamma=\frac{\beta g\Gamma}{\chi K_N^4}k_\perp^2.\tag{55}$$

Since $\Gamma>0$ due to the assumption of the negative temperature gradient, we must have $N^2<0$ for instability

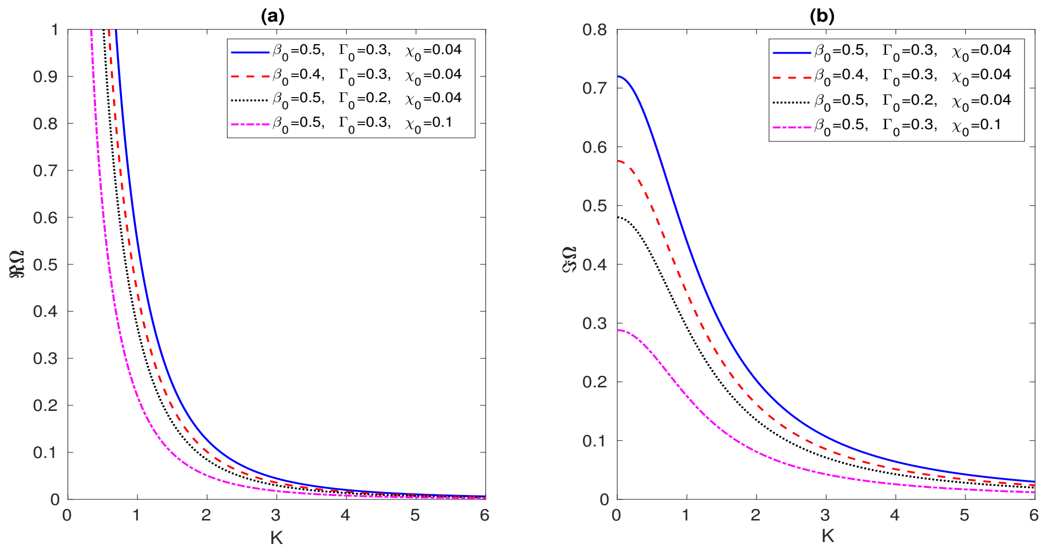


FIG. 1. The real [subplot (a)] and imaginary [subplot (b)] parts of the normalized wave frequency ($\Omega = \omega/\omega_g$), given by Eqs. (54) and (55), are plotted against the normalized wave number ($K = kL$) for different values of the parameters as in the legends. Here, $N^2 = -\omega_g^2 < 0$ and $L$ is the length scale of perturbations. The parameters are normalized as $\beta_0 = \beta T_0$, $\Gamma_0 = \Gamma L/T_0$, $\chi_0 = \chi/\omega_g L^2$, and $\nu_0 = \nu/\omega_g L^2$. Furthermore, $k_z = k\cos\theta$ and $k_\perp = k\sin\theta$ with $\theta$ denoting the angle between $k$ and $k_z$. The fixed parameter values are $\tilde{g} \equiv g/L\omega_g^2 = 0.4$, $\nu_0 = 0.05$, and $\theta = \pi/3$. The effect of $N^2$ is to reduce the instability growth rate (not shown).

to occur (See Sec. IV), and so Eq. (54) gives positive values of $\omega_r$. From Eqs. (54) and (55), it follows that both the wave frequency and the instability growth rate increase with increasing values of the thermal expansion coefficient, $\beta$ and the positive thermal lapse rate, $\Gamma$. In contrast, the thermal diffusivity effects significantly reduce the magnitudes of both $\omega_r$ and $\gamma$, since both vary inversely with $\chi$. Also, since the Brunt-Väisälä frequency contributes to $\omega_r$ and $\gamma$ in the orders of $1/|N^2|$ and $1/N^4$ respectively, it can influence both the wave frequency and the growth rate in reducing their values at higher values of $|N^2|$. It is interesting to note that both the wave frequency and the growth rate tend to decrease with increasing values of the wave number $k$ and reach steady states at higher values of $k$. The characteristics of the real ($\omega_r = \Re\omega$) and imaginary parts ($\gamma = \Im\omega$) are shown in Fig. 1 for different values of the parameters $\beta$, $\Gamma$, and $\chi$. From the subplots, it is evident that for the propagation of gravity waves, the wave number $k$ should not be too small or too large for which the wave frequency exceeds the magnitude of the Brunt-Väisälä frequency or it tends to vanish. Both the frequency and the instability growth rate attain maximum values at long-wavelength perturbations ($k \to 0$).

Nevertheless, the features, stated before, can be a bit different in a more general situation in which the sign and magnitude of $N^2$ could influence the onset of instability and the growth rates rather than the possibility of damping due to viscosity and diffusion effects. So, we consider the general dispersion equation (49) and solve it numerically. The results for the real and imaginary parts of the wave frequency are displayed in Fig. 2. We note that Eq. (49) can be considered as a quadratic equation in $\omega$, which gives two branches of complex wave modes. However, we consider the branch that gives positive values of both the real and imaginary parts of the wave frequency. From the subplots of Fig. 2, we find that both the real wave frequency and the growth rate can achieve maximum values in domains of long-wavelength perturbations. Such maximum values can be further enhanced even with a small reduction of the values of $|N^2|$ (not shown in the figure). It is also noted that while the growth rate can have a cut-off, the real wave frequency approaches more or less a constant at higher values of the wave number. Furthermore, in both the cases, the effects of the thermal expansion ($\beta$) and the temperature gradient ($\Gamma$) are to enhance the wave frequency and the growth rate with their increasing values (In agreement with the previous discussion at some particular cases). Because of their appearance in the dispersion equation (49), any one of the coefficients of the fluid viscosity ($\nu$) and the thermal diffusivity ($\chi$) can influence both the wave frequency ($\Re\omega$) and the instability growth rate ($\Im\omega$). While their effects on $\Re\omega$ are not significant [See the dash-dotted line in subplot (a)], the growth rate can be significantly reduced with increasing values of any one of $\chi$ and $\nu$. For brevity, we have only shown graphically the effects of $\chi$ on the characteristics of $\Re\omega$ and $\Im\omega$.

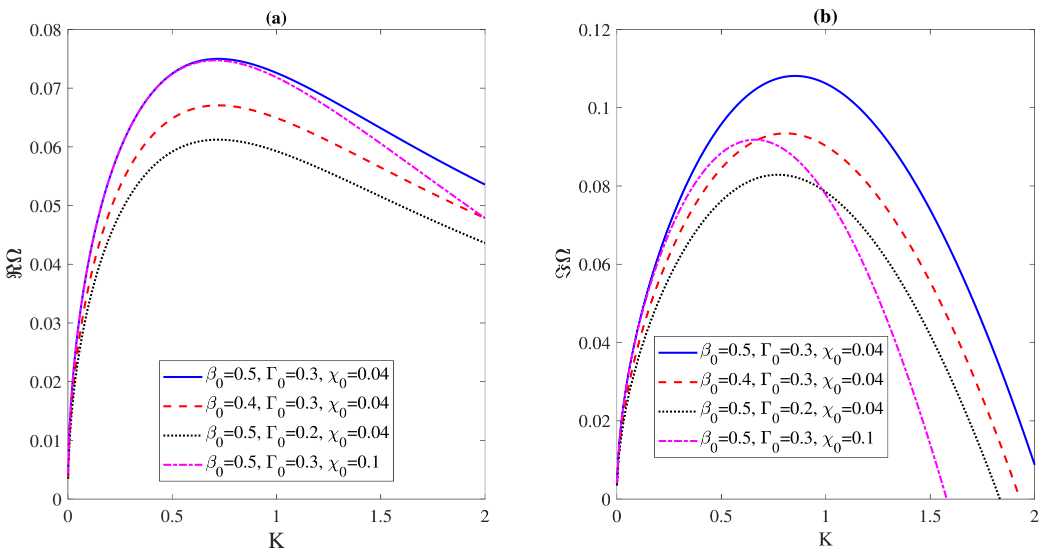


FIG. 2. The real [subplot (a)] and imaginary [subplot (b)] parts of the normalized wave frequency ($\Omega = \omega/\omega_g$), given by Eq. (49), are plotted against the normalized wave number ($K = kL$) for different values of the parameters as in the legends. Here, $N^2 = -\omega_g^2 < 0$ and $L$ is the length scale of perturbations. The parameters are normalized as $\beta_0 = \beta T_0$, $\Gamma_0 = \Gamma L/T_0$, $\chi_0 = \chi/\omega_g L^2$, and $\nu_0 = \nu/\omega_g L^2$. Furthermore, $k_z = k\cos\theta$ and $k_\perp = k\sin\theta$ with $\theta$ denoting the angle between $k$ and $k_z$. The fixed parameter values are $\tilde{g} \equiv g/L\omega_g^2 = 1.5$, $\nu_0 = 0.05$, and $\theta = \pi/3$. The effect of $N^2$ is to reduce the instability growth rate (not shown). The effects of the viscosity ($\nu$) on $\Re\omega$ and $\Im\omega$ are similar to $\chi$.

## VI. CONCLUSION

We have investigated the influence of the temperature-dependent density inhomogeneity due to thermal expansion on the stability of stratified fluids in the Earth's lower atmosphere ($0 < z < 50$ km) owing to its importance in the spatio-temporal evolution of perturbed flows. We show that modeling of such temperature dependence introduces a new factor involving the thermal expansion coefficient in the Brunt-Väisälä frequency and thus modifies its expression and the instability condition compared to those proposed in Ref. [8]. Furthermore, in contrast to Ref. [8], the instability of stratified flows can occur for $\beta\mathcal{T} < 1$ and $d\overline{T}/dz < 0$ only in the tropospheric region ($0 < z < 15$) km. At the stratospheric region ($15 < z < 50$) km, the fluid flow can be stable. It is also noted that the background temperature gradient, previously considered to vary, does not vary with atmospheric heights but remains a constant. We also consider the influence of the modified Brunt-Väisälä frequency, $N^2$ on the Rayleigh-Bénard convective flows and show that the negative temperature gradient for which the stratified flows associated with internal gravity waves become unstable can cause convective instability with an enhanced growth rate at a lower value of $N^2$. Such growth rates can be higher with increasing values of the thermal expansion coefficient and the thermal lapse rate, but can be significantly reduced by the effects of the thermal diffusion.

To conclude, the density inhomogeneity-driven thermal instability of stratified fluids relating to the Brunt-Väisälä frequency could be helpful for the initiation of large-scale (may be comparable to the turbulence or vortex phenomena) instabilities through the momentum and energy transfer such as those associated with internal gravity waves and acoustic-gravity waves in the atmosphere [11]. Furthermore, due to the Rayleigh-Bénard convective instability, a more efficient energy transfer between two layers in the atmosphere can take place by the effects of the thermal expansion and the temperature gradient, leading to a transition from laminar to turbulent flows [12, 13]. However, such efficient energy transport may eventually tend to resist some external perturbations, and the fluid flows may return to the equilibrium state. However, the detailed discussion concerning it is beyond the scope of the present study.

## AUTHOR DECLARATIONS

### Conflict of Interest

The authors have no conflicts to disclose.

### Author Contributions

**T. D. Kaladze:** Writing–original draft, Validation, Methodology, Investigation, Formal analysis, Conceptualization. **A. P. Misra:** Writing–review & editing, Validation, Software, Methodology, Investigation, Conceptualization.

## DATA AVAILABILITY STATEMENT

The data that support the findings of this study are available from the corresponding author upon reasonable request.


[1] F. H. Busse, Journal of Fluid Mechanics **82**, 794–794 (1977).

[2] D. J. Acheson and R. Hide, Reports on Progress in Physics **36**, 159 (1973).

[3] A. Tur and V. Yanovsky, Open Journal of Fluid Dynamics **3**, 64 (2013).

[4] A. Tur, M. Chabane, and V. Yanovsky, Open Journal of Fluid Dynamics **3**, 340 (2013).

[5] M. Kopp, A. Tur, and V. Yanovsky, Ukrainian Journal of Physics **66**, 478 (2021).

[6] B. R. Sutherland, Internal Gravity Waves (Cambridge University Press, 2010).

[7] E. Yiğit and A. S. Medvedev, Advances in Space Research **55**, 983 (2015).

[8] T. Kaladze and A. Misra, Physics Letters A **480**, 128990 (2023).

[9] L. Stenflo, Physics of Fluids **30**, 3297 (1987).

[10] T. D. Kaladze, A. P. Misra, A. Roy, and D. Chatterjee, Advances in Space Research **69**, 3374 (2022).

[11] I. Rogachevskii and N. Kleeorin, Physics of Fluids **36**, 026610 (2024), https://pubs.aip.org/aip/pof/article-pdf/doi/10.1063/5.0188732/19673481/026610_1_5.0188732.pdf.

[12] Y. Zhao, D. Wu, L. Duan, J. Wang, J. Li, L. Duan, and Q. Kang, Physics of Fluids **36**, 015132 (2024), https://pubs.aip.org/aip/pof/article-pdf/doi/10.1063/5.0173929/18626534/015132_1_5.0173929.pdf.

[13] M. Sharifi Ghazijahani and C. Cierpka, Physics of Fluids **36**, 035120 (2024), https://pubs.aip.org/aip/pof/article-pdf/doi/10.1063/5.0191403/19716786/035120_1_5.0191403.pdf.